CHIN.PHYS.LETT. Vol. 25, No. 4 (2008) 1220

Stochastic Simulation of Turing Patterns *

FU Zheng-Ping(傅正平)[1], XU Xin-Hang(徐昕航)[1], WANG Hong-Li(王宏利)[1,2,3**], OUYANG Qi(欧阳颀)[1,2,3]

[1]*School of Physics, Peking University, Beijing 100871*

[2]*Center for Theoretical Biology, Peking University, Beijing 100871*

[3]*The Beijing–Hongkong–Singapore Joint Center for Nonlinear and Complex Systems (PKU), Peking University, Beijing 100871*

(Received 20 November 2007)

We investigate the effects of intrinsic noise on Turing pattern formation near the onset of bifurcation from the homogeneous state to Turing pattern in the reaction–diffusion Brusselator. By performing stochastic simulations of the master equation and using Gillespie's algorithm, we check the spatiotemporal behaviour influenced by internal noises. We demonstrate that the patterns of occurrence frequency for the reaction and diffusion processes are also spatially ordered and temporally stable. Turing patterns are found to be robust against intrinsic fluctuations. Stochastic simulations also reveal that under the influence of intrinsic noises, the onset of Turing instability is advanced in comparison to that predicted deterministically.

PACS: 05. 45. −a, 05. 40. −a, 02. 50. −r

Turing pattern formation is a prototype of dissipative structures in systems driven far away from equilibrium. In reaction–diffusion systems, this spatially ordered and temporally static pattern is due to the destabilizing effect of diffusion from homogeneous states. It was firstly investigated by Alan Turing in his effort to explain the basis for biologic structures and patterns.[1] In recent years, intensive researches have been carried out on the mechanism involving in the formation of Turing pattern[2] and various other spatiotemporal patterns such as spiral waves, wave fronts and propagations. A variety of chemical media such as bistable, excitable, and oscillatory systems have been examined. The mathematical description of such pattern formations in chemical systems is often a set of non-linear partial differential equations in which the fluctuations have been averaged out. Nevertheless, noises have been frequently shown to play constructive roles in dynamic systems. They can change drastically the global behaviour of the system and lead to new phenomena which are not predicted by macroscopic differential equations. The effects of noise have been demonstrated in various situations such as noise-induced transitions[3]Horsthemke and stochastic resonance[4] in zero-dimensional systems, noise-induced phase transitions[5] and pattern formation[6] in spatially distributed systems, noise-induced fronts[7] and wave nucleation,[8] interaction of turbulence.[9] With only a few exceptions, most of the works have focused on the influence of external noises due to fluctuating environments. The effects of intrinsic noise which is inherent and unavoidable in reaction–diffusion systems have received much less attention.

In this Letter, we examine the role of intrinsic noise in Turing patterns. We are interested particularly in the influence of internal noise on the onset of Turing instability. In order to study the effect of internal noise in chemical systems, one has to resort to a more fundamental model, such as the approach of Langevin equation,[10,11] the chemical master equation formulation,[12] lattice-gas automata for reactive systems,[14] and the approach of microscopic simulation.[15]Bird Here we adopt the approach of direct stochastic simulations of the master equation for our purpose. We choose the Brusselator model, and examine the transition of the system from the homogeneous steady state to Turing pattern state. By using Gillespie's algorithm, we carry out stochastic simulations of the reaction and diffusion processes in a two-dimensional lattice. The results of simulation are compared with those from macroscopic reaction–diffusion rate equations. We show that the influence of intrinsic noise is significant in the vicinity of the Turing bifurcation point. Due to the effect of internal fluctuations, noisy Turing patterns can show up before the onset of Turing instability that is predicted by the rate equations. Particularly, the Turing pattern is robust against strong internal noise.

Stochastic simulation of spatially distributed systems would probably be inconvenient in the past because it would cost great deal of computer CPU time, but it is nowadays becoming practically applicable with the invent of fast computers. Mesoscopic investigations of Turing pattern formation in chemical systems has been investigated so far only with reactive lattice-gas automata by Kapral and his colleagues.[13] For our purpose, we adopt the Brusselator which is a

*Supported by the National Basic Research Programme of China under Grant Nos 2006CB910706 and 2007CB814800, the National Natural Science Foundation of China under Grant No 10774008, and the NFFTBS (J0630311).

**Email: hlwang@pku.edu.cn

© 2008 Chinese Physical Society and IOP Publishing Ltd

toy model that exhibits spiral waves and Turing patterns. It consists of the following four reaction steps,

$$R_1 : A \xrightarrow{k_1} U, \quad R_2 : \ B + U \xrightarrow{k_2} V + D,$$
$$R_3 : 2U + V \xrightarrow{k_3} 3U, \qquad R_4 : U \xrightarrow{k_4} E,$$

where k_i $(i = 1, 2, 3, 4)$ are rate constants, and the concentrations of A and B are constants and homogeneous so that the system is sustained far away from equilibrium. Both species U and V diffuse with diffusion constants D_u and D_v, respectively. The kinetic reaction–diffusion equations for the Brusselator model can be written as

$$\partial u/\partial t = a + u^2 v - (b + u) + D_u \Delta u, \tag{1}$$
$$\partial v/\partial t = bu - u^2 v + D_v \Delta v, \tag{2}$$

where u and v denote the concentrations of species U and V. In our simulations, we consider b as a control parameter, with other parameters fixed $a = 1$, $k_i = 1 (i = 1, 2, 3, 4)$, $D_u = 8.9$, $D_v = 71.1$. The system has the homogeneous steady state with $u_0 = a$, $v_0 = b/a$. Linear stability analysis around (u_0, v_0) yields that the steady state loses it stability and give way to Truing Pattern at the critical point $b_c = (1 + a\eta)^2, \eta = \sqrt{D_u/D_v}$[17]. With these parameters, the onset of Turing bifurcation locates at $b_c \approx 1.833$.

We perform stochastic simulations of the above reactions on a lattice. The basic idea of the approach is to divide the lattice into many spatial cells which are macroscopically small and microscopically large. Each cell is considered to be well-mixed, and is described by the numbers of reactive particles in it. The variables for each cell change as a result of two processes: chemical reactions, which are modelled by discrete Markov jumps, and diffusions whereby particles jump to an adjacent cell as Markov random walks. The time evolution of the stochastic system is then governed by the multivariate master equation. The master equation is overwhelmingly difficult for direct analysis. Therefore we resort to the approach of direct stochastic simulation. We assume that the species U and V react and diffuse stochastically on the two-dimensional lattice, which has been subdivided evenly into $N \times N$ square cells with size h. A cell on the lattice can be indexed as (i, j), and the populations of the dynamical species in the cell can be denoted as $U_{i,j}$ and $V_{i,j}$.

The constant Ω is introduced to measure the population size of the system.[19] It is the volume of the system effectively to determine the population scales of reacting species. Ω is also related with the microscopic reaction coefficient. When we perform stochastic simulation of the reactions R_1, R_2, R_3 and R_4, the microscopic reaction probabilities for the reactions are calculated from the macroscopic reaction rates k_1, k_2, k_3 and k_4 as k_1, k_2/Ω, k_3/Ω^2 and k_4. As the fewer the particles are contained in each cell, the more intensive the intrinsic fluctuation is, therefore by controlling the parameter Ω, the intrinsic noise strength can be adjusted.

When carrying out simulations, the stochastic simulation of the evolution of the reacting system is performed by repeatedly determining stochastically when and which individual reactions occur. As the computer time is linearly dependent on the total number of reaction channels when applying the original Gillspie's direct approach, the stochastic simulation would cost great deal of CPU time when the lattice of the system is large. In order to speed up Gillspie's algorithm, we organize the data of reaction probabilities into a tree.[18] The binary tree structure of data has been proven to be most efficient.[20] The second order Runge–Kutta method is adopted for the numerical integration of the partial differential equations (1) and (2). In both stochastic and deterministic simulations, the zero-flux-boundary condition is applied. In stochastic simulations, this condition is realized by forbidding the random diffusions of species U and V toward the outside of the boundaries.

For the purpose to characterize quantitatively the spatial pattern, we introduce an order parameter to measure the inhomogeneity of the pattern formation during its evolution, that is

$$\sigma = \sum_{i,j} \left(u_{i,j} - \frac{1}{N_x N_y} \sum_{i,j} u_{i,j} \right)^2. \tag{3}$$

As the system is stochastic and inherent fluctuations are always present, σ is not constant but an evolving and always fluctuating quantity even when the transient processes have died out. In our simulations, σ is also a criterion for judging whether the system has stochastically evolved to its asymptotic state. We find that it is enough when $\dfrac{d\sigma}{dt} < 4 \times 10^{-4} \mathrm{s}^{-1}$ for the stochastic dynamics to be asymptotic.

We first examine the Turing pattern formation at the level of mesoscopic description. From a homogeneous initial state, we simulate stochastically the system with parameters that lie beyond the point of Turing bifurcation. During the stochastic evolution, spots of Turing pattern turn up gradually. A snapshot of the pattern is depicted in Fig. 1(a). The spots scatter in the media with roughly equal distance from each other. Due to intrinsic fluctuations, the stochastic Turing pattern is not as regular as the strict hexagonal pattern obtained by direct numerical integration of Eq. (1) and (2). Figures 1(b)–1(c) demonstrate the diffusion flows of species U and V, respectively, on the lattice. The arrows indicate the direct of the flows, and the arrow length represents the flux. The inhibitor V diffuses much faster than the activator U because $D_v > D_u$. The narrowed regions where the species diffuse very slowly are recognized to be the

boundaries between the Turing spots. Both species diffuse much faster in the regions of spot than outside, while U diffuses away from and V diffuses into the centre of the spot. We find that at or near the boundary of a spot, the abundances of species U and V adopt roughly the homogeneous state. In order to sustain the balance between the fast diffusions in the region of spots, the third reaction step R_3 is found to occur much more frequently than the second reaction step R_2.

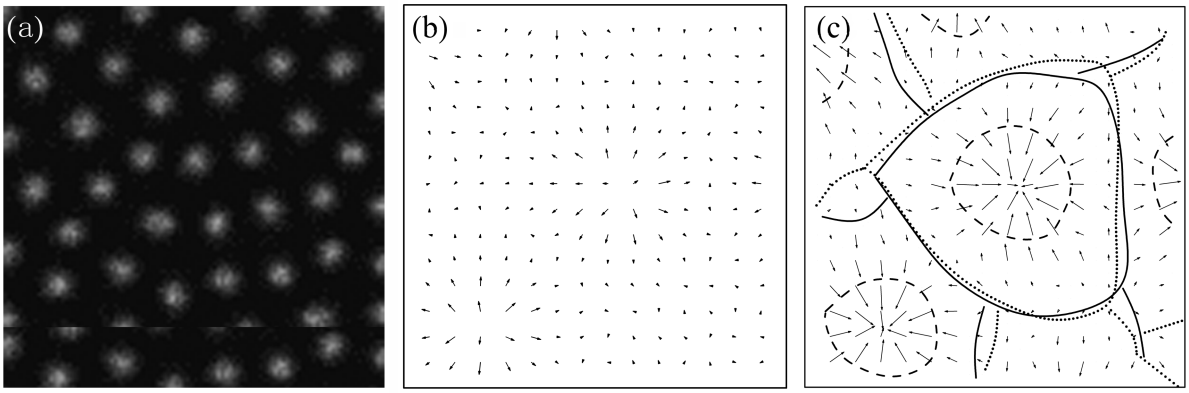


Fig. 1. (a) Snapshot of Turing pattern generated by encoding U field by grey scale, with white and black corresponding to high and low concentration, respectively. Here (b) and (c) show the diffusion flow vectors of species U and V, respectively; (c) shows that the net diffusive fluxes of V (also of U as can be seen in (b)) flow very slowly away in the neighbourhood of the solid and dotted lines. The closed lines circle spots of the pattern, where the diffusive fluxes achieve the maximal and the third reaction step occurs much more frequently than the second reaction step. Parameters: $b = 1.95$, $\Omega = 100$, lattice size $N = 100$.

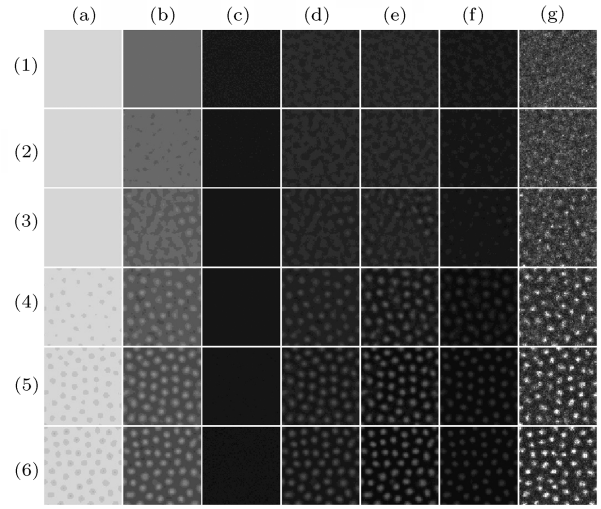


Fig. 2. Grey-scaled patterns of occurrence frequency for the reaction and diffusion processes as b is adjusted, with white and black corresponding to high-frequency and low-frequency respectively, for the parameters, i.e. Rows from (1) to (6): $b = 1.55, 1.65, 1.75, 1.85, 1.95, 2.05$, respectively; Columns (a) to (f) are in turn for the diffusions of species V and U, and R_1, R_2, R_3, R_4. Column (g) is for the concentration of U for the purpose of comparison. Other parameters: $\Omega = 20$, $N = 100$.

One of the merits of the stochastic simulation approach is that it allows one to check the occurrence frequencies of the reaction and diffusion processes. The pattern of occurrence frequency reveals how these processes corporate to sustain the spatially stable pattern of inhomogeneity. During the stochastic simulations, we have performed the frequency census for each of the processes in the system. We first check the situation with fixed $\Omega = 20$ and therefore definite strength of intrinsic noise. We adjust the control parameter b to scan it across the bifurcation point, and examine the patterns of the frequency distribution for the reactions and diffusions. The results are shown in Fig. 2. The data are processed after the system has evolved to its asymptotic state, and the frequencies of diffusions and reactions are then counted and encoded in grey scales. When the parameter b is larger than the critical value $b_c = 1.833$, as demonstrated in rows (4), (5), and (6) in Fig. 2, the patterns of occurrence frequency for the diffusion of V and U, and R_2, R_3, R_4 are closely similar to the patterns of U field (in column (g) and rows (4), (5), (6)), with the spots of occurrence overlapping with those of Turing pattern. The occurrence patterns for the diffusion of V (see first column in Fig. 2) are negative while the patterns for the processes of diffusion of U, and R_2, R_3, and R_4 are positive. The pattern for reaction R_1 is basically homogeneous because the species U is pumped onto the lattice at a constant rate. When b is decreased below b_c, as depicted in rows (1), (2), and (3) in Fig. 2, the spatial inhomogeneity in the patterns fades away. It is remarkable that even when $b < b_c$ the stochastic simulation of the system can still generate Turing patterns of low amplitude, as has been demonstrated in row (3) of Fig. 3 with $b = 1.75$. Even with larger distance from the deterministic bifurcation point ($b_c = 1.833$) when $b = 1.55$ (row (1)) and $b = 1.65$ (row (2)), the stochastically generated patterns still have spatial inhomogeneity. This is due to the influence of intrinsic

fluctuations.

In order to examine the influence of intrinsic noise on Turing pattern formation, we adjust the noise strength by varying the parameter of Ω. As the value of Ω is decreased, the populations of species U and V will fall down, and results in more intensive internal noises. Figure 3(A) demonstrates the dependence of σ on control parameter b when the value Ω adopts 100, 20, and 5, respectively. The order parameter σ is calculated when the system is asymptotic. The curve denoted by PDE is the deterministic result of Eqs. (1) and (2). With a large value of $\Omega = 100$ (asterisks in Fig. 3(A)), and when b is far away from b_c, stochastic simulations reveal that the system evolves into stable homogeneous state in which σ is close to zero. When b approaches b_c, σ grows gradually, while in contrast the deterministic transition is much sharper (open squares). The inhomogeneity is obvious even when $b = 1.75, 1.80$ ($< b_c$), implying the existence of Turing pattern before the onset of the bifurcation point predicted by Eq. (1) and (2). We see that due to the internal noise, the onset of transition to Truing pattern is advanced. Beyond b_c the stochastic results overlap roughly with the deterministic results with $\Omega = 10, 100$. With small value $\Omega = 5$ (triangles), σ is much larger as b is below b_c than with large Ω. The simulated Turing transition is vague as b crosses the onset of Turing instability.

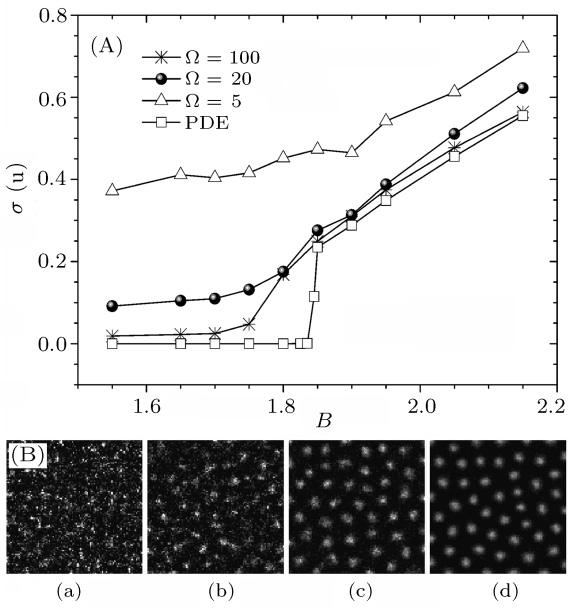


Fig. 3. (A) Behaviour of σ versus b as Ω is adjusted. The open squares are from stochastic simulations, and the other symbols are from partial differential equations (1) and (2). (B) Snapshots of Turing pattern encoded from U field simulated stochastically with different Ω. Parameters: $b = 2.05$, $\Omega = 2$ for (a), $\Omega = 5$ for (b), $\Omega = 20$ for (c), and $\Omega = 100$ for (d).

Figure 3(B) depicts the asymptotic snapshots of U field when Ω grows from 2, to 5, 20, and 100, respectively. From our stochastic simulations, the averaged particle number of species U or V in a cell is about 5.2 for (a), 13.7 for (b), 56.0 for (c), and 281.3 for (d), respectively. As the abundances grow, the intrinsic noise strength is decreased, and the patterns become clearer and more ordered. With $\Omega = 5$ (panel (b) in Fig. 3(B)), the mean particle number is quite small, and the Turing pattern is obviously supported under the influence of intensive intrinsic noise. We can see that the Turing pattern is quite robust against inherent strong fluctuations. This finding is in agreement with the results of lattice-gas automata reported by Kapral's group.[13]

In summary, we have simulated stochastically the chemical master equation for the Brusselator model at the neighbourhood of Turing bifurcation. Our stochastic simulations demonstrated that the spatial patterns of occurrence frequency for the reaction and diffusion processes are also Turing-like, and that it is their corporation that produce the Turing pattern. Simulations demonstrated that Turing pattern can survive and is robust to intensive inherent fluctuations. We find that even when the particle numbers of reaction species are just above 10, the Turing pattern can still be supported. This finding might be significant for the formation of biological patterns and structures where the abundances of biological macromolecules are typically very small. Under the influence of intrinsic noises, the onset of Turing instability is advanced in comparison to that predicted by the deterministic rate equations.

References

[1] Turing A M 1952 *Trans. R. Soc. London* B **237** 37
[2] Cross M C and Hohenberg P C 1993 *Rev. Mod. Phys.* **65** 851
[3] Horsthemke W and Lefever R 1984 *Noise-Induced Transitions* (Berlin: Springer)
[4] Gammaitoni L, Hanggi P, Jung P and Marchesoni F 1998 *Rev. Mod. Phys.* **70** 233
[5] Van den Broeck C, Parrondo J M and Toral R 1994 *Phys. Rev. Lett.* **73** 3395
[6] Buceta J et al 2003 *Phys. Rev.* E **67** 021113
[7] Santos M A and Sancho J M 1999 *Phys. Rev.* E **59** 98
[8] Jung P and Mayer-Kress G 1995 *Phys. Rev. Lett.* **74** 2130
[9] Wang H and Ouyang Q 2002 *Phys. Rev.* E **65** 046206
Wang H 2004 *Phys. Rev. Lett.* **93** 154101
Wang H and Ouyang Q 2005 *Chaos* **15** 023702
[10] Nitzan A, Ortoleva P, Deutch R and Ross J 1974 *J. Chem. Phys.* **61** 1056
[11] Hochberg D et al 2006 *Phys. Rev.* E **73** 066109
[12] Nicolis G and Prigogine I 1977 *Self-Organization in Nonequilibrium Systems* (New York: Wiley-Interscience)
[13] Voroney J et al 1996 *Physica* D **99** 303
[14] Boon J P et al 1996 *Phys. Rep.* **273** 55
[15] Bird G A 1976 *Molecular Gas Dynamics* (Oxford: Clarendon)
[16] Gillespie D 1977 *J. Phys. Chem.* **81** 2340
[17] Peña B and Perez-Garcia C 2001 *Phys. Rev.* E **64** 056213
[18] Gibson M A and Bruck J 2000 *J. Phys. Chem.* A **104** 1876
[19] Gillespie D T 1976 *J. Comput. Phys.* **22** 402
[20] Matthias W 2003 *Phy. Rev.* E **68** 036213